Voltage-controlled moiré potentials, propagation and luminescence of indirect excitons in $MoSe_2/WSe_2$ heterostructure

L. H. Fowler-Gerace*, Zhiwen Zhou, D. J. Choksy, and L. V. Butov
Department of Physics, University of California at San Diego, La Jolla, California 92093-0319, USA
*lefowler@physics.ucsd.edu

Abstract: We present a new mechanism for exciton transport control based on tuning moiré potentials by voltage to enable delocalization, present long-range exciton propagation due to this mechanism, explore correlations between exciton luminescence and propagation properties.

Excitonic devices based on controlled propagation of spatially indirect excitons (IXs), also known as interlayer excitons, are demonstrated in GaAs structures but limited to low temperatures due to low IX binding energies [1]. IXs in transition metal dichalcogenide (TMD) structures are characterized by high binding energies [2,3] offering the opportunity for high-temperature operation. However, strong moiré superlattice potentials in TMD structures [4,5] localize IXs, making IX propagation different in TMD and GaAs structures. A relatively short-range IX propagation with 1/e IX luminescence decay distances $d_{1/e}$ up to ~3 μm was observed in TMD structures [6-8]. In earlier excitonic devices, IX transport was controlled by an energy barrier to IX propagation created by the gate electrode [1,7,8]. In this work, we present a new mechanism for exciton transport control. It is based on tuning the moiré potentials by voltage to enable exciton delocalization. We present the long-range IX propagation due to this mechanism with $d_{1/e} >$ 10 μm in a TMD heterostructure. We also explore correlations between IX luminescence and propagation properties.

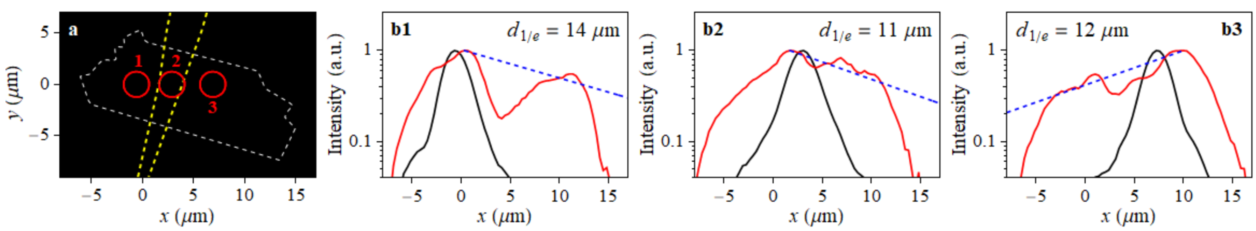

Figure 1: (a) The white and yellow dashed lines show the boundaries of $MoSe_2/WSe_2$ heterostructure and graphene gate, respectively. Circles 1, 2, and 3 correspond to the position of laser excitation in panels b1, b2, and b3, respectively. (b1-b3) Normalized IX luminescence profiles along y = 0 for V_g = 10 V (red) and V_g = 0 (black). Dashed lines show exponential signal reduction with indicated 1/e decay distances, $d_{1/e}$. P = 4 mW.

We study IXs in a $MoSe_2/WSe_2$ van der Waals TMD heterostructure assembled by stacking mechanically exfoliated 2D crystals on a graphite substrate. IXs are formed by electrons and holes confined in adjacent $MoSe_2$ and WSe_2 monolayers encapsulated by hBN [9]. The bias across the structure is created by the gate voltage V_g applied between the semitransparent multilayer graphene top gate and the global graphite back gate (Fig. 1a). IXs are generated by laser excitation focused in region 1, 2, or 3 (Fig. 1a). T = 2 K in the experiments.

The predicted strong moiré superlattice potentials [4,5] in the $MoSe_2/WSe_2$ heterostructure are expected to localize IXs. At V_g = 0, IX propagation is suppressed (Fig. 1b), consistent with the IX localization. Increasing V_g enables the IX propagation away from the excitation spot for any excitation spot position on the heterostructure, with $d_{1/e} > 10$ μm (Fig. 1b). We traced the IX spectra along the propagation path and verified that the propagating signal corresponds to the IX luminescence. A lower IX luminescence intensity is seen in the region covered by the graphene gate.

In contrast to earlier excitonic devices [1,7,8], IX transport is not controlled by an energy barrier to IX propagation created by the gate electrode but is controlled in the entire heterostructure and for any excitation spot position on the heterostructure. The theory [5] predicts that the moiré potential is tuned by voltage in TMD heterostructures and increasing electric field can reduce the moiré potential amplitude and can energetically align the potential energy minima at different sites of the moiré supercell, thus causing percolation of IX states through the structure. The tuning of the moiré potential can cause the observed long-range IX propagation with applied voltage. A comparison with the theory [5] can be complicated by factors including, for instance, a possible atomic reconstruction changing the potential landscape.

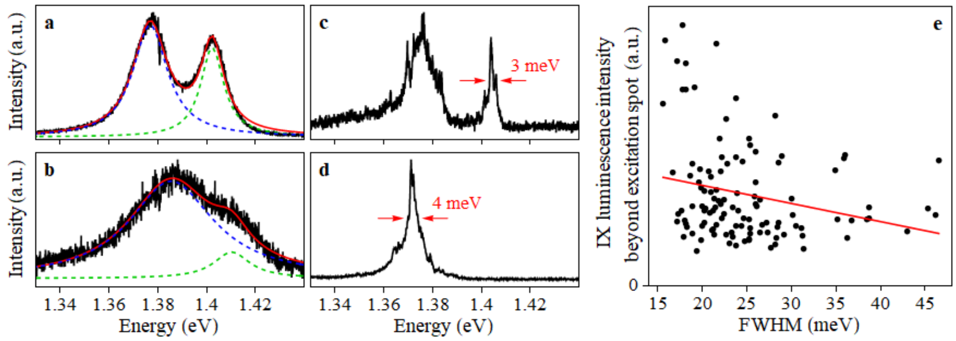

Figure 2: (a,b) IX luminescence spectra at position (6,0) (a) and (1,2) (b). The coordinates are in μm, the map is in Fig. 1a. $P = 4$ mW. (c,d) Spectra at the position of the narrowest neutral (c) and charged (d) IX linewidth. The coordinates are (11,-2) and (6,0), respectively. $P = 5$ μW. (e) Correlation between IX linewidth in the excitation spot and spectrally integrated IX intensity beyond the excitation spot, in the area between 2 and 4 μm from the center of the 2 μm excitation spot, for 1x1 μm pixels of the heterostructure map in Fig.1a. The line is a linear fit. $P = 4$ mW. $V_g = 0$.

Besides the moiré potential, samples have disorder potential due to the heterostructure imperfections. The disorder potential also contributes to the IX localization and suppresses the IX propagation. The long-range propagation indicates the small disorder for IX transport scattering in the device.

We explored a relation between IX luminescence and propagation properties in the regime of suppressed propagation at $V_g = 0$ (the studies at applied voltage in the long-range propagation regime form the subject for future work). Two IX lines are observed (Fig. 2) whose energy splitting and temperature dependence identify them as neutral and charged IXs [10]. A map of IX luminescence reveals regions of broad and narrow IX linewidths, representative spectra are shown in Fig. 2a,b. With reducing laser excitation power P, the linewidths of both lines reduce reaching the narrowest 3 meV for neutral (Fig. 2c) and 4 meV for charged (Fig. 2d) IXs, then the lines break to sets of narrower lines within the envelopes given by these linewidths. These narrow 3 and 4 meV linewidths for the sets of neutral and charged IX states indicate a small disorder in the device, consistent with the realization of the long-range IX propagation (Fig. 1).

Even at $V_g = 0$, some suppressed IX propagation is observed. It is characterized by the IX luminescence intensity beyond the excitation spot. Figure 2e indicates that the heterostructure regions with smaller IX linewidth show greater IX propagation. The correlation coefficient indicates that the correlation is significant. This shows that heterostructure imperfections, which lead to the broadening of IX luminescence linewidth, also suppress IX propagation.

These studies were supported by DOE Office of Basic Energy Sciences under award DE-FG02-07ER46449. The heterostructure fabrication and data analysis were supported by NSF grant 1905478.

[1] A.A. High, E.E. Novitskaya, L.V. Butov, M. Hanson, A.C. Gossard, Control of exciton fluxes in an excitonic integrated circuit, Science 321, 229 (2008).

[2] M.M. Fogler, L.V. Butov, K.S. Novoselov, High-temperature superfluidity with indirect excitons in van der Waals heterostructures, Nat. Commun. 5, 4555 (2014).

[3] T. Deilmann, K.S. Thygesen, Interlayer trions in the MoS_2/WS_2 van der Waals heterostructure, Nano Lett. 18, 1460 (2018).

[4] F. Wu, T. Lovorn, A.H. MacDonald, Topological Exciton Bands in Moiré Heterojunctions, Phys. Rev. Lett. 118, 147401 (2017).

[5] H. Yu, G.-B. Liu, J. Tang, X. Xu, W. Yao, Moiré excitons: From programmable quantum emitter arrays to spin-orbit-coupled artificial lattices, Sci. Adv. 3, e1701696 (2017).

[6] L.A. Jauregui, A.Y. Joe, K. Pistunova, D.S. Wild, A.A. High, Y. Zhou, G. Scuri, K. De Greve, A. Sushko, C.-H. Yu, T. Taniguchi, K. Watanabe, D.J. Needleman, M.D. Lukin, H. Park, P. Kim, Electrical control of interlayer exciton dynamics in atomically thin heterostructures, Science 366, 870 (2019).

[7] D. Unuchek, A. Ciarrocchi, A. Avsar, Z. Sun, K. Watanabe, T. Taniguchi, A. Kis, Valley-polarized exciton currents in a van der Waals heterostructure, Nat. Nanotechnol. 14, 1104 (2019).

[8] Y. Liu, K. Dini, Q. Tan, T. Liew, K.S. Novoselov, W. Gao, Electrically controllable router of interlayer excitons, Sci. Adv. 6, eaba1830 (2020).

[9] L.H. Fowler-Gerace, D.J. Choksy, L.V. Butov, Voltage-controlled long-range propagation of indirect excitons in a van der Waals heterostructure, Phys. Rev. B 104, 165302 (2021).

[10] E.V. Calman, L.H. Fowler-Gerace, D.J. Choksy, L.V. Butov, D.E. Nikonov, I.A. Young, S. Hu, A. Mishchenko, A.K. Geim, Indirect excitons and trions in $MoSe_2/WSe_2$ van der Waals heterostructures, Nano Lett. 20, 1869 (2020).